Screening by deep sequencing reveals mediators of microRNA tailing in *C. elegans*

Katherine Prothro*[1,3], Karl-Frédéric Vieux*[1], Cameron Palmer[1,4], Isana Veksler-Lublinsky[2], Katherine McJunkin[1,5]

[1]National Institutes of Diabetes and Digestive and Kidney Diseases Intramural Research Program, Bethesda, MD 20815 USA
[2]Ben Gurion University of the Negev, Beer Sheva 8410501 Israel
[3]Present address: Stanford University School of Medicine, Stanford, CA 94305 USA
[4]Present address: National Cancer Institute, Rockville, MD 20850 USA
[5]To whom correspondence should be addressed: Tel: +1-301-496-6991; Fax: +1-301-496-5239 ; Email: mcjunkin@nih.gov
*The authors wish it to be known that, in their opinion, the first two authors should be regarded as joint First Authors.

Abstract

microRNAs are frequently modified by addition of untemplated nucleotides to the 3' end, but the role of this tailing is often unclear. Here we characterize the prevalence and functional consequences of microRNA tailing *in vivo,* using the *C. elegans* model. MicroRNA tailing in *C. elegans* consists mostly of mono-uridylation of mature microRNA species, with rarer mono-adenylation which is likely added to microRNA precursors. Through a targeted RNAi screen, we discover that the TUT4/TUT7 gene family member CID-1/CDE-1/PUP-1 is required for uridylation, whereas the GLD2 gene family member F31C3.2 is required for adenylation. Thus, the TUT4/TUT7 and GLD2 gene families have broadly conserved roles in miRNA modification. We specifically examine the role of tailing in microRNA turnover. We determine half-lives of microRNAs after acute inactivation of microRNA biogenesis, revealing that half-lives are generally long (median=20.7h), as observed in other systems. Although we observe that tails are more prevalent on older microRNAs, disrupting tailing does not alter microRNA abundance or decay. Thus, tailing is not a global regulator of decay in *C. elegans*. Nonetheless, by identifying the responsible enzymes, this study lays the groundwork to explore whether tailing plays more specialized context- or miRNA-specific regulatory roles.

Introduction

microRNAs (miRNAs) are small non-coding RNAs that bind Argonaute (Ago) proteins to form the miRNA-induced silencing complex (miRISC), which represses complementary target mRNAs (1). miRNA-target interactions are important in sculpting gene regulation for normal physiology (2).

Canonical miRNAs are derived from longer primary transcripts (pri-miRNAs) from which a hairpin-like secondary structure is recognized and excised by the Microprocessor complex, made up of the

ribonuclease Drosha and its protein cofactor DGCR8/Pasha (3). This excised hairpin, known as the miRNA precursor (or pre-miRNA), is exported to the cytoplasm where its loop is cleaved by Dicer (3). One strand of the resulting miRNA duplex is then preferentially loaded into Ago, and the passenger strand is degraded (3).

In contrast to biogenesis, the process of miRNA turnover is poorly understood, despite turnover's equivalent importance in determining miRNA abundance. In general, miRNA half-lives are long, on the order of ~20h, with some miRNAs exhibiting characteristically shorter half-lives (4–8). Certain physiological signals and developmental contexts can accelerate miRNA turnover by poorly understood mechanisms, such as neuronal activity which globally destabilizes miRNAs in the retina (9).

Untemplated nucleotide additions to the 3' end ("tailing") can regulate both biogenesis and decay of miRNAs through multiple mechanisms. These modifications are carried out by a class of enzymes known as terminal nucleotidyl transferases (TENTs), which also have other roles in regulating mRNAs and viral genomes (10, 11).

The most well-understood examples of tailing regulating miRNAs involve uridylation of miRNA precursors. This type of tailing generally impacts atypical precursors that lack the canonical 2-nt single-stranded 3' overhang which is generated by Microprocessor cleavage and recognized by Dicer (12). The type of uridylation and its consequence depends on the length of the 3' overhang, where 1-nt overhangs are mono-uridylated to favor biogenesis and further recessed ends are oligo-uridylated resulting in decay of the precursor (12). Precursor uridylation can also regulate biogenesis by shifting the site of Dicer cleavage, which can result in alternative miRNA guide strand selection (arm-switching) (13). Oligo-uridylation and decay of the *let*-7 precursor is induced even in the context of a canonical 2-nt 3' overhang by binding of the RNA-binding protein LIN-28 (14, 15). Finally, non-canonical Microprocessor-independent miRNA precursors derived from short introns (mirtron precursors) are also highly uridylated, inhibiting their biogenesis in *Drosophila* (16, 17).

Tailing can also occur on mature miRNAs, again with a wide variety of outcomes. Target RNAs with extensive complementarity cause the 3' end of miRNAs to be tailed and trimmed, concomitant with miRNA destabilization (18–20). This process, known as target-directed miRNA degradation (TDMD), is induced by a handful of known naturally-occurring triggers, including tissue-specific lncRNAs and viral small RNAs that target a host miRNA (21–27). While tailing was initially assumed to be causative of miRNA decay in this context, recent studies demonstrate examples in which tailing is dispensable for TDMD, suggesting that 3' tailing may be a symptom of miRNA 3' end display rather than an upstream regulatory event in TDMD (27–31).

In other contexts, tailing of mature miRNAs is necessary for sequence-non-specific miRNA turnover. During embryonic development of Drosophila, fish, and mice, terminal adenylation of maternally-contributed miRNAs induces their turnover at the maternal to zygotic transition (32).

Conversely, terminal adenylation of mature miRNAs is stabilizing and activating for miR-122 and a subset of other miRNAs (33–35). Finally, 3' miRNA tailing can even alter target repertoire (36). Overall, tailing of miRNA precursors and mature miRNAs have a wide range of regulatory consequences. How tailing is coupled to these various outcomes in a miRNA- and context-dependent manner is not understood.

In this work, we set out to examine the role of tailing in miRNA turnover in a model organism *in vivo*. We first use deep sequencing and meta-analysis of published data to characterize miRNA tailing in *C. elegans*. We perform a candidate RNAi screen by deep sequencing to discover the enzymes responsible for tailing, demonstrating that terminal uridylyltransferase 4 (TUT4)/TUT7 ortholog caffeine induced death homolog 1 (CID-1) is required for U-tailing, and defective in germ line development 2 (GLD2) ortholog F31C3.2 - here named GLD-2-related 2 (GLDR-2) – is responsible for A-tailing. Finally, we use acute inactivation of miRNA biogenesis to measure miRNA turnover and show that, while U-tailing increases as miRNAs age, this is correlative not causative of miRNA turnover. Overall, this work importantly defines ancestral functions of TENT families that modify miRNAs, and – by defining the required enzymes – lays the groundwork for future studies to determine whether miRNA tailing in *C. elegans* may play context-dependent or miRNA-specific functions.

Methods

C. elegans Maintenance and RNAi

N2 (wild type) and SX1137 (*pash-1(mj100)* I) worms were maintained at 15°C. For RNA samples, L1s were synchronized by alkaline hypochlorite lysis of gravid adults followed by hatching in M9 with 1mM cholesterol at 15°C for 48-72h. L1s were plated on NGM seeded with either OP50 or RNAi bacteria and maintained at 15°C until early day one of gravid adulthood (until just a few embryos were laid on the plate, ~76h after plating). This time point was harvested for N2 samples, SX1137 samples in the RNAi screen, and served as 0h in time courses involving SX1137. Additional SX1137 plates were shifted to 25°C, and samples were collected at the indicated time points after upshift for time courses on OP50 or RNAi.

RNAi plates were supplemented with 1µg/ml IPTG and 1µg/ml Carbenicillin (and poured no more than two weeks prior to use and stored at 4°C). The RNAi bacteria (HT115 expressing an RNAi vector) were prepared from single clones derived from the Ahringer library (Source Bioscience), the Vidal library

(Source Bioscience), or custom RNAi vectors (Table S1). All previously-reported RNAi phenotypes were observed. Furthermore, a robust RNAi response in each sample was confirmed by the presence of abundant siRNAs mapping to the targeted locus.

Small RNA Sequencing

Total RNA was isolated by Trizol extraction. Spike-ins were added at a final concentration of 0.1pg/µl (OP50 samples) or 1pg/µl (RNAi samples) in 100ng/µl total RNA. See Table S2 for spike-in information. For each sample, 600ng of RNA was used for input, and libraries were prepared using the NEBNext Small RNA Library Prep set for Illumina with the following modifications. The first size selection was performed after the RT reaction by excising 65-75nt cDNA from an 8% denaturing acrylamide gel. PCR products were again size selected using a Pippin prep or 6% native acrylamide gel. Input RNA and final library sample quality were assessed using a Bioanalyzer. Equimolar amounts of each library were pooled; up to 24 indexed samples were pooled together for sequencing.

Data analysis

Deep sequencing data were analyzed using the miTRATA web interface (37) after preprocessing the data using miTRATA's accompanying Python3-based preprocess.seq pipeline, installed on the NIH High Performance Computing Cluster in a dedicated miniconda environment. The mature *C. elegans* miRNAs from miRBase Release 22.1 (38) were used for miTRATA mapping. A custom C++ script reformatted the miTRATA output by consolidating read numbers for all reads meeting the following criteria into a tabular format: a tail:head ratio > 0.12 (16) and a tail length ≤ 3nt. These reformatted tailing data were further analyzed in RStudio. (One non-unique miRNA pair was of sufficient abundance to be included in tailing analysis – *mir-44/45-3p*; *mir-45-3p* was therefore culled from tabular data to avoid plotting this data twice.) To calculate reads per million, reads were normalized by the number of genome-mapping reads in the library (Table S3). The number of genome-mapping reads was determined using Bowtie (39) to align to the *C. elegans* genome (WS215), with the arguments -v 3 -f -B 1 -a --best --strata. Alignments were then filtered based on the length of the reads and the number of mismatches as follows: for sequence lengths 16-17, 18-19, 20-24, or >24: zero, one, two, or three mismatches were allowed, respectively. Reads passing this threshold were considered "genome-mapping reads". A custom bash/R pipeline was used to calculate trimming relative to canonical miRNA length from the miTRATA output files.

Statistical Analysis

Fisher's exact test for enrichment of tailing on 3p- or 5p-derived miRNAs was performed by counting miRNAs as above or below 1% tailed, and pooling these counts from three biological replicates to generate

the contingency table, which was analyzed in GraphPad QuickCalcs. For the RNAi screen, GraphPad Prism v8.4.3 was used to perform one-way repeated measures ANOVA followed by Dunnett's multiple comparison test. All RNAi conditions were compared to an empty vector sample, and this comparison was repeated for each empty vector sample. RNAi conditions that were significant in comparison to each empty vector sample are highlighted, with the least significant p-value reported. All miRNAs >50RPM in all empty vector replicates were analyzed. To determine miRNA half-lives, for each miRNA with >50 RPM at 0h in both replicates, fold change at each time point relative to 0h was calculated using spike-in-normalized reads. GraphPad Prism v8.4.3 was used to fit a one phase decay non-linear regression model with the following constraints: Y0=1, Plateau=0, K>0.

Phylogenetic analysis

MEGA-X (40) was used to build phylogenetic trees of orthologous genes (to CID-1 and PUP-2, or to GLD-2 and F31C3.2) identified in WormBase ParaSite version WBPS15 (41). Orthologs from select non-nematode species were included as shown (Figures S5 and S7). The classification of nematode species into clades was downloaded from the same WormBase Parasite version WBPS15. Additional trees containing only *C. elegans* genes and common model organisms are shown in Figures 2 and 3. All alignments were generated using Clustal W (Multiple Alignment Gap Opening Penalty=10, Gap Extension Penalty=0.2, Negative Matrix Off, Delay Divergent Cutoff 30%). Maximum Likelihood method was used in MEGA-X, with no test of phylogeny, JTT model of substitution, uniform rates among sites, no subsetting ("use all sites"), NNI, automatic initial tree, and no branch swap filter.

Results

Patterns of miRNA tailing in *C. elegans* suggest different substrates than in flies and vertebrates

To determine the nature and prevalence of miRNA tailing in *C. elegans*, we first cloned and deep sequenced small RNAs from wild type animals. To ensure reliable measurements of tailing, only miRNAs with greater than 50 reads per million were included in tailing analysis. To determine the level of background in our sequencing and computational pipeline, ten synthetic miRNAs (whose sequences are endogenous to plants and not present in *C. elegans* – Table S2) were spiked in to purified total RNA before preparation for deep sequencing. Although these RNA species were never present in the context of cellular lysate, up to 1% tailing was detected; therefore, tailing levels measured below 1% (delineated by dashed line on all tailing plots) are low confidence and could arise due to PCR or sequencing errors.

Most tailing consisted of a single nucleotide addition (Figure 1A). Tails of two or more nucleotides were much rarer, and so we focused our analysis on further characterization of the single-nucleotide tails. Three replicates of adult animals showed strong correlation in rates of tailing (Figure S1). Modest levels of miRNA tailing were observed, and tailing in *C. elegans* consisted primarily of uridylation with a much lower frequency of adenylation (Figure 1B, Table S4). This is in contrast to humans and flies, where both adenylation and uridylation are prevalent (42–45). In addition, a single miRNA, *mir-83-3p*, was highly cytidylated in all replicates (Figure 1B, Figure S1), a modification that is rarely observed in animals, but was recently reported as a frequent addition to plant miRNA precursors (46).

Either the mature miRNA species or the miRNA precursor may be the substrate of the observed tailing. If the vast majority of observed tailing events occur on miRNA precursors, then miRNAs derived from the 3' arm of the precursor hairpin (3p) would be expected to bear more terminal additions than those derived from the 5' arm of the hairpin (5p) since the 3' end of the 5p arm is not accessible for tailing prior to Dicer-mediated cleavage (Figure 1C). In vertebrates and *Drosophila*, miRNA precursors are the primary substrate of uridylation, though mature miRNAs can also be uridylated (29, 42–44, 47). In contrast, 3p and 5p miRNAs displayed similar levels of uridylation in *C. elegans* (Figure 1D), indicating that U-tailing likely predominantly occurs on mature miRNA species. Untemplated adenylation generally occurs on mature miRNAs in vertebrates, and a modest 3p bias suggests that both precursor and mature miRNAs are adenylation substrates in *Drosophila* (42–44). In contrast, A-tailing in *C. elegans* shows a strong bias, occurring primarily on 3p-derived miRNAs (Figure 1D), suggesting that A-tailing in *C. elegans* occurs predominantly on miRNA precursors.

Because global developmentally-regulated tailing has been demonstrated in other models (32), we examined published datasets from developmental time courses to determine whether tailing of *C. elegans* miRNAs is correlated with any particular developmental stage (48–50). No consistent global differences in rates of uridylation or other types of tailing were observed (Figure 1E and Figure S2A, Table S5). We were especially interested in oocyte and early embryo samples since miRNA adenylation is highly prevalent in these time points and leads to turnover of maternally-contributed miRNAs in other species (32), but neither adenylation nor uridylation was globally dynamic during the course of early embryonic development in *C. elegans* (Figure S2B, Table S5) (51).

miRNA uridylation requires CID-1

To determine what role tailing may play in regulating miRNAs in *C. elegans*, we next set out to identify the enzymes responsible for these modifications. To this end, we performed RNAi against a list of candidate terminal nucleotidyl transferases (TENTs). For each knockdown, we performed deep sequencing of small RNAs, and compared the proportion of tailed isoforms to those in three biological replicates of

empty vector. Of RNAi against 18 candidate tailing enzymes, only the RNAi targeting *cid-1* significantly abrogated miRNA U-tailing (p-value = 0.0003, Figure 2A-B, Figure S3, Table S6), and this was reproduced in independent experiments (Figure S4A). Though *cid-1(lf)* was previously reported to reduce miRNA U-tailing (52), our study allows for the comparison of the relative contributions of all putative TENTs, demonstrating that other TENTs are not required. In particular, knockdown of *pup-2*, a paralog of *cid-1*, does not affect miRNA terminal uridylation (Figure 2B). Although CID-1 and PUP-2 are redundant in their biological function of protecting germline fate (53), they do not appear to be redundant for this molecular function, since *cid-1* knockdown alone has a strong effect.

Both CID-1 (also known as PUP-1 or CDE-1) and PUP-2 are orthologs of TUT4 and TUT7, which act redundantly, along with TENT2/TUT2/GLD2, to uridylate miRNA precursors in mammals (12, 15, 54). CID-1 and PUP-2 are much less similar (17.4%) than TUT4 and TUT7 (44.5%), consistent with the lack of redundancy of CID-1 and PUP-2 for miRNA uridylation in *C. elegans*. The common ancestor of nematodes and vertebrates likely contains only one TUT4/7 family gene, and a recent duplication occurred in each lineage to give rise to two paralogs (Figure 2C) (10). The duplication in nematodes likely occurred in the common ancestor of Rhabditina or earlier (Figure S3). In contrast, the *Drosophila* lineage has lost this gene family (10). Overall, the role of CID-1 demonstrates that the function of the TUT4/7 gene family in uridylation of miRNA species is deeply conserved, though the substrate specificity shows a different bias (preferentially targeting mature miRNAs rather than precursors in *C. elegans*) (Figure 2C).

miRNA adenylation requires F31C3.2

We also analyzed the RNAi screen of putative TENTs to identify enzymes required for adenylated miRNA species, with the goal of assessing whether adenylation affects processing or stability of miRNAs. Because of the generally low level of A tailing and the noise inherent in tailing levels below 1%, we highlight those miRNAs that were >1% adenylated in empty vector samples in Figure 3. Knockdown of F31C3.2 reduced A-tailing of these miRNAs (p-value = 0.0003, Figure 3A-B, Figure S6) in multiple replicates (Figure S4B).

F31C3.2 is in the TENT2/GLD2 gene family of non-canonical cytoplasmic poly(A) polymerases, and we therefore name it GLD-2-related 2 (GLDR-2) (Figure 3C). The common ancestor of *Bilateria* likely had a single GLD2 gene, and duplications have occurred in the *Nematoda* lineage (GLD-2 and F31C3.2/ GLDR-2) and the *Drosophila* lineage (GLD2 and WISPY) (10). The nematode duplication likely occurred in the common ancestor of clades III-V or earlier (Figure S7). The single GLD2 gene in mammals and the paralog WISPY in *Drosophila* both catalyze adenylation of mature miRNAs (32, 33, 35, 43). Here we show that the paralog F31C3.2/GLDR-2 - rather than GLD-2 itself - adenylates miRNAs in *C. elegans*, though the enrichment of this modification on 3p-derived miRNAs suggests that precursors rather than mature

miRNAs are the substrate of F31C3.2/GLDR-2. Although F31C3.2/GLDR-2 previously had no known function *in vivo,* a high throughput assay in yeast showed that the enzyme is indiscriminate with respect to substrate nucleotide (55). However, knockdown of F31C3.2/GLDR-2 only affects the prevalence of A tailing (and not C, G, or U additions) in our *in vivo* experiments. Thus, additional factors in the *C. elegans* cellular context may confer nucleotide substrate specificity to F31C3.2/GLDR-2.

RNAi screen does not identify nucleases targeting tailed miRNAs

In many previous studies, tailed miRNA precursors or tailed mature miRNAs are targeted to specific nucleases (56–59). To determine whether tailed miRNAs are the substrate of a specific nuclease, we also performed RNAi against a panel of nucleases previously implicated in miRNA turnover (4, 56, 57, 60–63). We observed only subtle effects on tailing (Figure 2A, 3A, S3 and S6). Although RNAi against exosome component *exos-4* showed statistically significant differences in U tailing compared to the vector control (p-value = 0.016), the effect was a slight decrease in tailed species, suggesting an indirect effect of the RNAi. (The direct effect of knocking down an exonuclease that targets tailed miRNAs would be an increase in the prevalence of tailing.) Overall, these data suggest that tailed miRNAs are not specifically targeted to any of the examined nucleases (Note that PARN-1 was not included since previous studies showed no effect of *parn-1(lf)* on miRNA tailing or stability in *C. elegans* (64).) Overall, we have not observed evidence for the role of any of these nucleases in the trimming of tailed miRNAs.

miRNAs are relatively long-lived

Having identified the enzymes required for miRNA tailing in *C. elegans*, we sought to examine the potential involvement of tailing in regulating miRNA turnover. To this end, we first characterized miRNA turnover in *C. elegans* by measuring miRNA half-lives using a system in which miRNA biogenesis can be acutely inactivated: a temperature-sensitive allele of the DGCR8 homolog *pash-1* (65). Upon upshift to restrictive temperature, *pash-1(ts)* no longer processes new miRNAs, and the decay of existing miRNAs can be observed over time (Figure 4A) (65, 66). To measure miRNA decay, we collected time course samples 0, 6, 24, and 48 hours after upshift to restrictive temperature. Because miRNAs comprise a large portion of the small RNA complement and global miRNA levels will change over the time course after *pash-1* inactivation, synthetic miRNAs not present in the *C. elegans* genome were spiked in to the samples at a constant concentration relative to total RNA to allow for robust normalization. Adult animals shifted to restrictive temperature produced a few non-viable progeny and did not proliferate further, so dilution of miRNAs by increasing amounts of total RNA is minimal in this system. After normalization to spike-ins, global decay of miRNAs was observed over the 48h time course in two biological replicates (Figure 4B, Table S7).

Using spike-in-normalized reads, time course data were fit to exponential decay curves to calculate miRNA half-lives. Half-lives determined using data from only one replicate were well correlated between replicates (Figure S8A). Therefore, we used data from both replicates together to fit half-life values with greater confidence. The fit of the decay curves was best when deep sequencing data were normalized to spike-ins, as expected, significantly outperforming normalization to total mapped reads (Figure S8B). Data for miRNAs with half-lives longer than the 48h course of the experiment (14 out of 68 analyzed miRNAs) generally did not fit the exponential decay curve well (Figure S8C, Table S8). In contrast, shorter-lived miRNAs fit the curve well, with 40 out of 54 miRNAs having a fit with $R^2 > 0.8$ (Figure 4C, Figure S8C, Table S8). Overall, miRNAs were fairly stable, with a median half-life of 20.7h (Figure 4D, Table S8), similar to most observations in mammalian and *Drosophila* cells (4, 6–8, 67). These results using spike-in normalization and deep sequencing yield longer half-lives than a previous study using *pash-1(ts)* (Figure S8D) (65). The previous study employed microarray miRNA quantification and normalization to non-miRNA small RNAs (siRNA and mirtron); when our data were normalized to mirtron reads, we observed a similar range of half-lives to their study (Figure S8E). This suggests that mirtron or siRNA normalization does not effectively control for library-wide changes. Nonetheless, both studies highlighted similar sets of fast-decaying miRNAs, with *mir-61*, *mir-71, mir-253*, and *mir-250* among the six lowest half-lives in both datasets (Table S8) (65).

miRNA tailing and trimming correlate with miRNA age

Previous studies have demonstrated that terminal modifications correlate with miRNA turnover (18, 19, 22, 26, 27). These studies demonstrated that miRNAs that are targeted for decay display high levels of 3' tailing. In our datasets, as miRNAs turn over during the time course after PASH-1 inactivation, the ensemble of miRNAs becomes increasingly skewed towards older miRNAs (approaching turnover). To determine whether miRNA terminal modifications are associated (correlatively or causatively) with miRNA turnover in our dataset, we quantified tailing across the time course. We observed that indeed later time points displayed higher levels of uridylation (Figure 5A-B, Table S7). This global trend included a large increase in tailing for *mir-70-3p* and many other miRNAs, although not all miRNAs displayed increased tailing over the time course (Figure 5C, Table S7). The increase of U-tailing on aging miRNAs is consistent with the mature miRNA being a substrate of U-tailing as suggested above (Figure 1C). No change was observed in adenylation of miRNAs over the time course (Figure 5A), consistent with its substrate being miRNA precursors.

Like tailing, 3' trimming is also often observed concomitant with tailing (18, 22). Therefore, we also analyzed trimming over the time course after PASH-1 inactivation. Like tailing, global 3' trimming increased in later time points, as indicated by a lower proportion of canonical-length reads and increased

proportion of shorter genome-matching reads (Figure S9). Like tailing, this subtle global trend was more apparent when examining individual miRNAs (Figure S9). Thus, both tailing and trimming increase in older miRNAs that are approaching turnover.

Since U-tailing is increasing over the course of turnover, we next asked whether tailing is correlated with the rate of miRNA turnover. We did not observe an overall correlation between initial prevalence of the U-tailed isoform and half-life for a given miRNA (Figure S10A), nor between rate of increase in tailing and half-life (Figure S10B). While this indicates that terminal uridylation is unlikely to be the primary determinant of turnover, uridylation might play a modulatory role that is not apparent in bulk analysis due to larger effects of other unknown parameters.

Abrogation of miRNA tailing does not affect miRNA turnover

To determine whether uridylation may play a modulatory role - either stimulating or impairing turnover - we sought to disrupt miRNA tailing and then measure rates of miRNA turnover in its absence. In wild type animals, disrupting U-tailing by *cid-1* RNAi did not change abundance of miRNAs, suggesting that turnover is unchanged (Figure 6A). To further examine the effect of tailing on miRNA decay, we profiled abbreviated time courses after PASH-1 inactivation in the *pash-1(ts)* background (0 and 24h after upshift). RNAi against *cid-1* reduced U-tailing at both time points (Figure S11A, Table S9). However, when we examined the change in miRNA abundance from zero to 24h after PASH-1 inactivation, *cid-1* RNAi did not have a global effect (Figure 6B). We also specifically examined miRNAs that show high increases in uridylation after *pash-1* inactivation to determine whether these cases might be particularly sensitive to disrupting uridylation by *cid-1* RNAi. For these miRNAs, tailing was disrupted but turnover was not reproducibly altered (Figure 6C). A small number of miRNAs that were not characterized by high tailing did show reproducibly higher $\log_2$fold change in *cid-1* RNAi than vector control (Figure 6B, highlighted in Figure S11A-B). However, this is likely due to a lower starting amount of these miRNAs in T0 *cid-1* RNAi samples (Figure S11C); indeed these miRNAs are the only ones with less than half the abundance in *cid-1* RNAi T0 samples as compared to vector T0 samples. Furthermore, both strands of the miRNA duplex derived from these precursors behaved similarly, supporting an effect of *cid-1* RNAi on transcription or biogenesis rather than on decay rate of the mature miRNA species (Figure S11D). Because these miRNAs are largely germline and embryo-specific (49, 68), the difference in their abundance most likely corresponds to slight differences in staging of *cid-1* RNAi T0 samples due to pleiotropic effects of *cid-1(lf),* which negatively impacts germline function and embryo production (53). Taken together, these data show that miRNA uridylation in *C. elegans* is not a global regulator of miRNA decay.

Next, we examined whether A-tailing altered miRNA abundance or turnover. In wild type, although F31C3.2/*gldr-2* RNAi reduces A-tailing, RNAi did not alter miRNA abundance (Figure S11E). In the *pash-*

1(ts) setting, fewer miRNAs could be examined with high confidence due to lower abundance and/or lower A-tailing. (Lower miRNA abundance may be the result of reduction of *pash-1* function even at permissive temperature, and likewise, a reduced lifetime of miRNA precursors in this setting could lead to reduced A-tailing.) Nonetheless, we still observed that F31C3.2/*gldr-2* RNAi abrogated A-tailing in the 24h time point, (Figure S11F, Table S9). When examining the change in miRNA abundance from zero to 24h after temperature shift, F31C3.2/*gldr-2* RNAi did not affect the rate of miRNA decay (Figure S11G). Therefore, the adenylation mediated by F31C3.2/GLDR-2 does not regulate miRNA abundance or stability.

High levels of mirtron uridylation do not affect abundance

Mirtrons are non-canonical miRNAs that derive from small introns; debranching of these intron lariats results in a miRNA precursor-like hairpin structure, bypassing the requirement for Microprocessor-mediated cleavage (69, 70). Previous work showed that mirtron precursors are highly uridylated and that, in *Drosophila*, this uridylation is carried out by the *Drosophilidae*-specific TUTase6-related enzyme Tailor and negatively regulates mirtron abundance (10, 16, 17, 71). In wild type sequencing libraries, only one mirtron, *mir-62*, was abundant enough for reliable tailing analysis. However, in *pash-1(ts)* libraries at restrictive temperature, mirtrons are relatively elevated in sequencing libraries since they do not depend on Microprocessor activity, while canonical miRNAs are globally depleted. This allowed for the analysis of tailing of multiple mirtrons. We observed that (as previously reported from aggregate sequencing data), 3p-derived mirtrons are highly uridylated to a much greater degree than canonical miRNAs, with the exception of *mir-62* (Figure S11H) (71). Not only is *mir-62* atypical in its proportion of tailing, but *mir-62* is also much more abundant than the other mirtrons (Figure S11H). Like uridylation of canonical miRNAs, uridylation of mirtrons also required CID-1 (Figure S11H). Surprisingly, although knockdown of *cid-1* strongly abrogated mirtron tailing, the abundance of the mirtrons was not elevated as was observed in *Drosophila* (upon knockdown of Tailor) (Figure S11H). Therefore, although the high rate of U tailing is conserved for most *C. elegans* mirtrons, this modification does not regulate mirtron abundance.

Discussion

In this work, we characterize the nature of miRNA tailing in *C. elegans*, with the broad view of determining ancestral functions of this class of post-transcriptional modification. We show that uridylation is far more prevalent than adenylation in *C. elegans*, unlike mammals and Drosophila in which both modifications are common (42–45).

We show that the substrate of these additions is shifted in different lineages. Based on its even distribution between 3p- and 5p-derived miRNAs, we infer that uridylation targets mature miRNAs in *C. elegans*, whereas precursors are the predominant substrate in mammals and *Drosophila* (29, 42–44, 47). In contrast, adenylation is skewed towards 3p-derived miRNAs in *C. elegans*, indicating that miRNA precursors are its likely substrate, unlike in vertebrates where mature miRNAs are more often adenylated and *Drosophila* where both precursors and mature miRNAs are likely substrates (42–44).

Despite the shifts in the apparent substrate of the modification, the enzymes required for these modifications are largely conserved. MiRNA uridylation requires CID-1, which is in the same TUT-4/7 gene family that carries out this modification (along with TUT2/GLD2) in mammals (12, 15, 54). MiRNA adenylation requires F31C3.2/GLDR-2. F31C3.2/GLDR-2 is in the TUT2/GLD2/PAPD-4 gene family which carries out miRNA adenylation in mammals and *Drosophila* (32, 33, 35, 43). Importantly, the enzymatic activities of these enzymes in uridylation/adenylation has been previously demonstrated *in vitro* or in a heterologous tethering assay (52, 55).

We characterize rates of miRNA decay in *C. elegans*, which are largely similar to those in other organisms (4, 6–8, 67). The median half-life – 20.7h – is relatively long, and strikingly long in considering the context of the *C. elegans* life cycle time scale. Half-lives in this study may even be slightly underestimated due to slight expansion of the culture after upshift to restrictive temperature. This perdurance of miRNAs across a large portion of the *C. elegans* life span is consistent with the idea that many miRNAs may serve to specify and maintain differentiation of cell types, rather than acting as dynamic switches regulating transient developmental states (2).

Nonetheless, certain miRNAs (especially *mir-61*, *mir-71, mir-253*, and *mir-250*) are reproducibly short-lived across replicates in our study and previous studies (65). How these fast decay rates are specified will be an important area of ongoing study. Moreover, we have only analyzed a single condition; decay may be differentially regulated for subsets of miRNAs in distinct developmental stages or under stress conditions. Notably, a study conducted in L1 stage larvae highlighted different fast-decaying miRNAs than our study in adults (72), supporting the notion that miRNA turnover is developmentally regulated and may be critical for the miRNAs' biological functions (73–78).

Although we observed that the proportion of tailed species increased as miRNAs age, disrupting tailing had no impact on turnover. This is consistent with recent kinetic analysis which demonstrated that tailing is faster than 3' trimming, so miRNAs are more likely to carry a tail as they age (8). TDMD is the most frequently-studied context in which tailing correlates with decay, yet recent work on TDMD suggests that tailing is correlative – not causative – of TDMD, and that conformational changes that promote decay of the Argonaute-miRNA complex also expose the miRNA 3' end to TENTs (27, 28, 30, 31). However, in

specific developmental contexts, tailing does promote wholesale miRNA turnover (32). Therefore, cell-type or developmental contexts which we have not yet examined may also couple decay to tailing in *C. elegans*. By identifying the enzymes required for miRNA tailing, this study lays the groundwork for discovering and dissecting such regulation.

Data Availability

All raw sequence data will be deposited in NCBI Sequence Read Archive (BioProject Number PRJNA703306). Reviewer link:
https://dataview.ncbi.nlm.nih.gov/object/PRJNA703306?reviewer=2h12a5i72qildfkt3l259bdli9

Funding

This work was funded by the NIDDK Intramural Research Program (ZIA DK075147).

Acknowledgments

We thank the NIDDK Genomics Core and NIH High Performance Computing. Strains are regularly received from the CGC, which is funded by NIH Office of Research Infrastructure Programs (P40 OD010440). Thank you to Eleanor Maine and members of the McJunkin lab for helpful discussions.

References

1. Dexheimer,P.J. and Cochella,L. (2020) MicroRNAs: From Mechanism to Organism. *Front. Cell Dev. Biol.*, **8**.
2. Alberti,C. and Cochella,L. (2017) A framework for understanding the roles of miRNAs in animal development. *Dev.*, **144**, 2548–2559.
3. Ha,M. and Kim,V.N. (2014) Regulation of microRNA biogenesis. *Nat. Rev. Mol. Cell Biol.*, **15**, 509–24.
4. Bail,S., Swerdel,M., Liu,H., Jiao,X., Goff,L.A., Hart,R.P. and Kiledjian,M. (2010) Differential regulation of microRNA stability. *RNA*, **16**, 1032–1039.
5. Rissland,O.S., Hong,S.-J. and Bartel,D.P. (2011) MicroRNA destabilization enables dynamic regulation of the miR-16 family in response to cell-cycle changes. *Mol. Cell*, **43**, 993–1004.
6. Marzi,M.J., Ghini,F., Cerruti,B., De Pretis,S., Bonetti,P., Giacomelli,C., Gorski,M.M., Kress,T., Pelizzola,M., Muller,H., *et al.* (2016) Degradation dynamics of microrna revealed by a novel pulse-chase approach. *Genome Res.*, **26**, 554–565.
7. Reichholf,B., Herzog,V.A., Fasching,N., Manzenreither,R.A., Sowemimo,I. and Ameres,S.L. (2019) Time-Resolved Small RNA Sequencing Unravels the Molecular Principles of MicroRNA Homeostasis. *Mol. Cell*, **75**, 756-768.e7.
8. Kingston,E.R. and Bartel,D.P. (2019) Global analyses of the dynamics of mammalian microRNA metabolism. *Genome Res.*, 10.1101/gr.251421.119.
9. Krol,J., Busskamp,V., Markiewicz,I., Stadler,M.B., Ribi,S., Richter,J., Duebel,J., Bicker,S., Fehling,H.J., Schübeler,D., *et al.* (2010) Characterizing light-regulated retinal microRNAs reveals rapid turnover as a common property of neuronal microRNAs. *Cell*, **141**, 618–631.
10. Modepalli,V. and Moran,Y. (2017) Evolution of miRNA Tailing by 3′ Terminal Uridylyl Transferases in Metazoa. *Genome Biol. Evol.*, **9**, 1547–1560.
11. De Almeida,C., Scheer,H., Zuber,H. and Gagliardi,D. (2018) RNA uridylation: a key posttranscriptional modification shaping the coding and noncoding transcriptome. *Wiley Interdiscip. Rev. RNA*, **9**.
12. Kim,B., Ha,M., Loeff,L., Chang,H., Simanshu,D.K., Li,S., Fareh,M., Patel,D.J., Joo,C. and Kim,V.N. (2015) TUT7 controls the fate of precursor microRNAs by using three different uridylation mechanisms. *EMBO J.*, **34**, 1801–1815.
13. Kim,H., Kim,J., Yu,S., Lee,Y.Y., Park,J., Choi,R.J., Yoon,S.J., Kang,S.G. and Kim,V.N. (2020) A Mechanism for microRNA Arm Switching Regulated by Uridylation. *Mol. Cell*, **78**, 1224-1236.e5.
14. Heo,I., Joo,C., Cho,J., Ha,M., Han,J. and Kim,V.N. (2008) Lin28 mediates the terminal uridylation of let-7 precursor MicroRNA. *Mol. Cell*, **32**, 276–284.
15. Heo,I., Joo,C., Kim,Y.-K.K., Ha,M., Yoon,M.-J.J., Cho,J., Yeom,K.-H.H., Han,J. and Kim,V.N. (2009) TUT4 in concert with Lin28 suppresses microRNA biogenesis through pre-microRNA uridylation. *Cell*, **138**, 696–708.
16. Reimão-Pinto,M.M., Ignatova,V., Burkard,T.R., Hung,J.H., Manzenreither,R.A., Sowemimo,I., Herzog,V.A., Reichholf,B., Fariña-Lopez,S. and Ameres,S.L. (2015) Uridylation of RNA Hairpins by Tailor Confines the Emergence of MicroRNAs in Drosophila. *Mol. Cell*, **59**, 203–216.
17. Bortolamiol-Becet,D., Hu,F., Jee,D., Wen,J., Okamura,K., Lin,C.J., Ameres,S.L. and Lai,E.C. (2015) Selective Suppression of the Splicing-Mediated MicroRNA Pathway by the Terminal Uridyltransferase Tailor. *Mol. Cell*, **59**, 217–228.
18. Ameres,S.L., Horwich,M.D., Hung,J.-H., Xu,J., Ghildiyal,M., Weng,Z. and Zamore,P.D. (2010) Target RNA-directed trimming and tailing of small silencing RNAs. *Science*, **328**, 1534–1539.
19. Baccarini,A., Chauhan,H., Gardner,T.J., Jayaprakash,A.D., Sachidanandam,R. and Brown,B.D. (2011) Kinetic analysis reveals the fate of a microRNA following target regulation in mammalian cells. *Curr. Biol.*, **21**, 369–376.
20. de la Mata,M., Gaidatzis,D., Vitanescu,M., Stadler,M.B., Wentzel,C., Scheiffele,P., Filipowicz,W. and Grosshans,H. (2015) Potent degradation of neuronal miRNAs induced by highly complementary targets. *EMBO Rep.*, **16**, 500–511.
21. Cazalla,D., Yario,T., Steitz,J.A. and Steitz,J. (2010) Down-regulation of a host microRNA by a

Herpesvirus saimiri noncoding RNA. *Science*, **328**, 1563–6.
22. Marcinowski,L., Tanguy,M., Krmpotic,A., Rädle,B., Lisnić,V.J., Tuddenham,L., Chane-Woon-Ming,B., Ruzsics,Z., Erhard,F., Benkartek,C., *et al.* (2012) Degradation of cellular mir-27 by a novel, highly abundant viral transcript is important for efficient virus replication in vivo. *PLoS Pathog.*, **8**, e1002510.
23. Libri,V., Helwak,A., Miesen,P., Santhakumar,D., Borger,J.G., Kudla,G., Grey,F., Tollervey,D. and Buck,A.H. (2012) Murine cytomegalovirus encodes a miR-27 inhibitor disguised as a target. *Proc. Natl. Acad. Sci. U. S. A.*, **109**, 279–284.
24. Piwecka,M., Glažar,P., Hernandez-Miranda,L.R., Memczak,S., Wolf,S.A., Rybak-Wolf,A., Filipchyk,A., Klironomos,F., Cerda Jara,C.A., Fenske,P., *et al.* (2017) Loss of a mammalian circular RNA locus causes miRNA deregulation and affects brain function. *Science*, **357**, eaam8526.
25. Ghini,F., Rubolino,C., Climent,M., Simeone,I., Marzi,M.J. and Nicassio,F. (2018) Endogenous transcripts control miRNA levels and activity in mammalian cells by target-directed miRNA degradation. *Nat. Commun.*, **9**, 3119.
26. Bitetti,A., Mallory,A.C., Golini,E., Carrieri,C., Carreño Gutiérrez,H., Perlas,E., Pérez-Rico,Y.A., Tocchini-Valentini,G.P., Enright,A.J., Norton,W.H.J., *et al.* (2018) MicroRNA degradation by a conserved target RNA regulates animal behavior. *Nat. Struct. Mol. Biol.*, **25**, 244–251.
27. Kleaveland,B., Shi,C.Y., Stefano,J. and Bartel,D.P. (2018) A Network of Noncoding Regulatory RNAs Acts in the Mammalian Brain. *Cell*, **174**, 350-362.e17.
28. Sheu-Gruttadauria,J., Pawlica,P., Klum,S.M., Wang,S., Yario,T.A., Schirle Oakdale,N.T., Steitz,J.A. and MacRae,I.J. (2019) Structural Basis for Target-Directed MicroRNA Degradation. *Mol. Cell*, **75**, 1243-1255.e7.
29. Yang,A., Shao,T.J., Bofill-De Ros,X., Lian,C., Villanueva,P., Dai,L. and Gu,S. (2020) AGO-bound mature miRNAs are oligouridylated by TUTs and subsequently degraded by DIS3L2. *Nat. Commun.*, **11**.
30. Han,J., LaVigne,C.A., Jones,B.T., Zhang,H., Gillett,F. and Mendell,J.T. (2020) A ubiquitin ligase mediates target-directed microRNA decay independently of tailing and trimming. *Science*, **370**, eabc9546.
31. Shi,C.Y., Kingston,E.R., Kleaveland,B., Lin,D.H., Stubna,M.W. and Bartel,D.P. (2020) The ZSWIM8 ubiquitin ligase mediates target-directed microRNA degradation. *Science*, **370**, eabc9359.
32. Lee,M., Choi,Y., Kim,K., Jin,H., Lim,J., Nguyen,T.A.A., Yang,J., Jeong,M., Giraldez,A.J.J., Yang,H., *et al.* (2014) Adenylation of maternally inherited microRNAs by Wispy. *Mol. Cell*, **56**, 696–707.
33. Katoh,T., Sakaguchi,Y., Miyauchi,K., Suzuki,T., Kashiwabara,S.-I., Baba,T. and Suzuki,T. (2009) Selective stabilization of mammalian microRNAs by 3' adenylation mediated by the cytoplasmic poly(A) polymerase GLD-2. *Genes Dev.*, **23**, 433–8.
34. Burns,D.M., D'Ambrogio,A., Nottrott,S. and Richter,J.D. (2011) CPEB and two poly(A) polymerases control miR-122 stability and p53 mRNA translation. *Nature*, **473**, 105–108.
35. D'Ambrogio,A., Gu,W., Udagawa,T., Mello,C.C. and Richter,J.D. (2012) Specific miRNA stabilization by Gld2-catalyzed monoadenylation. *Cell Rep.*, **2**, 1537–45.
36. Yang,A., Bofill-De Ros,X., Shao,T.J., Jiang,M., Li,K., Villanueva,P., Dai,L. and Gu,S. (2019) 3′ Uridylation Confers miRNAs with Non-canonical Target Repertoires. *Mol. Cell*, **75**, 511-522.e4.
37. Patel,P., Ramachandruni,S.D., Kakrana,A., Nakano,M. and Meyers,B.C. (2016) miTRATA: a web-based tool for microRNA Truncation and Tailing Analysis. *Bioinformatics*, **32**, 450–452.
38. Kozomara,A. and Griffiths-Jones,S. (2014) MiRBase: Annotating high confidence microRNAs using deep sequencing data. *Nucleic Acids Res.*, **42**, D68–D73.
39. Langmead,B., Trapnell,C., Pop,M. and Salzberg,S.L. (2009) Ultrafast and memory-efficient alignment of short DNA sequences to the human genome. *Genome Biol.*, **10**, R25.
40. Kumar,S., Stecher,G., Li,M., Knyaz,C. and Tamura,K. (2018) MEGA X: Molecular evolutionary genetics analysis across computing platforms. *Mol. Biol. Evol.*, **35**, 1547–1549.
41. Bolt,B.J., Rodgers,F.H., Shafie,M., Kersey,P.J., Berriman,M. and Howe,K.L. (2018) Using WormBase ParaSite: An integrated platform for exploring helminth genomic data. In *Methods in Molecular Biology*. Humana Press Inc., Vol. 1757, pp. 471–491.

42. Chiang,H.R., Schoenfeld,L.W., Ruby,J.G., Auyeung,V.C., Spies,N., Baek,D., Johnston,W.K., Russ,C., Luo,S., Babiarz,J.E., *et al.* (2010) Mammalian microRNAs: experimental evaluation of novel and previously annotated genes. *Genes Dev.*, **24**, 992–1009.
43. Burroughs,A.M., Ando,Y., de Hoon,M.J., Tomaru,Y., Nishibu,T., Ukekawa,R., Funakoshi,T., Kurokawa,T., Suzuki,H., Hayashizaki,Y., *et al.* (2010) A comprehensive survey of 3' animal miRNA modification events and a possible role for 3' adenylation in modulating miRNA targeting effectiveness. *Genome Res.*, **20**, 1398–1410.
44. Berezikov,E., Robine,N., Samsonova,A., Westholm,J.O., Naqvi,A., Hung,J.H., Okamura,K., Dai,Q., Bortolamiol-Becet,D., Martin,R., *et al.* (2011) Deep annotation of Drosophila melanogaster microRNAs yields insights into their processing, modification, and emergence. *Genome Res.*, **21**, 203–215.
45. Wyman,S.K., Knouf,E.C., Parkin,R.K., Fritz,B.R., Lin,D.W., Dennis,L.M., Krouse,M.A., Webster,P.J. and Tewari,M. (2011) Post-transcriptional generation of miRNA variants by multiple nucleotidyl transferases contributes to miRNA transcriptome complexity. *Genome Res.*, **21**, 1450–1461.
46. Song,J., Wang,X., Song,B., Gao,L., Mo,X., Yue,L., Yang,H., Lu,J., Ren,G., Mo,B., *et al.* (2019) Prevalent cytidylation and uridylation of precursor miRNAs in Arabidopsis. *Nat. Plants*, **5**, 1260–1272.
47. Thornton,J.E., Du,P., Jing,L., Sjekloca,L., Lin,S., Grossi,E., Sliz,P., Zon,L.I. and Gregory,R.I. (2014) Selective microRNA uridylation by Zcchc6 (TUT7) and Zcchc11 (TUT4). *Nucleic Acids Res.*, **42**, 11777–11791.
48. Batista,P.J., Ruby,J.G., Claycomb,J.M., Chiang,R., Fahlgren,N., Kasschau,K.D., Chaves,D.A., Gu,W., Vasale,J.J., Duan,S., *et al.* (2008) PRG-1 and 21U-RNAs Interact to Form the piRNA Complex Required for Fertility in C. elegans. *Mol. Cell*, **31**, 67–78.
49. Kato,M., de Lencastre,A., Pincus,Z. and Slack,F.J. (2009) Dynamic expression of small non-coding RNAs, including novel microRNAs and piRNAs/21U-RNAs, during Caenorhabditis elegans development. *Genome Biol.*, **10**, R54.
50. Shi,Z., Montgomery,T.A., Qi,Y. and Ruvkun,G. (2013) High-throughput sequencing reveals extraordinary fluidity of miRNA, piRNA, and siRNA pathways in nematodes. *Genome Res.*, **23**, 497–508.
51. Stoeckius,M., Maaskola,J., Colombo,T., Rahn,H.-P., Friedländer,M.R., Li,N., Chen,W., Piano,F. and Rajewsky,N. (2009) Large-scale sorting of C. elegans embryos reveals the dynamics of small RNA expression. *Nat. Methods*, **6**, 745–751.
52. van Wolfswinkel,J.C., Claycomb,J.M., Batista,P.J., Mello,C.C., Berezikov,E. and Ketting,R.F. (2009) CDE-1 Affects Chromosome Segregation through Uridylation of CSR-1-Bound siRNAs. *Cell*, **139**, 135–148.
53. Li,Y. and Maine,E.M. (2018) The balance of poly(U) polymerase activity ensures germline identity, survival and development in caenorhabditis elegans. *Dev.*, **145**.
54. Heo,I., Ha,M., Lim,J., Yoon,M.-J., Park,J.-E., Kwon,S.C., Chang,H. and Kim,V.N. (2012) Mono-uridylation of pre-microRNA as a key step in the biogenesis of group II let-7 microRNAs. *Cell*, **151**, 521–532.
55. Preston,M.A., Porter,D.F., Chen,F., Buter,N., Lapointe,C.P., Keles,S., Kimble,J. and Wickens,M. (2019) Unbiased screen of RNA tailing activities reveals a poly(UG) polymerase. *Nat. Methods*, **16**, 437–445.
56. Chang,H.M., Triboulet,R., Thornton,J.E. and Gregory,R.I. (2013) A role for the Perlman syndrome exonuclease Dis3l2 in the Lin28-let-7 pathway. *Nature*, **497**, 244–248.
57. Ustianenko,D., Hrossova,D., Potesil,D., Chalupnikova,K., Hrazdilova,K., Pachernik,J., Cetkovska,K., Uldrijan,S., Zdrahal,Z. and Vanacova,A. (2013) Mammalian DIS3L2 exoribonuclease targets the uridylated precursors of let-7 miRNAs. *RNA*, **19**, 1632–1638.
58. Yoda,M., Cifuentes,D., Izumi,N., Sakaguchi,Y., Suzuki,T., Giraldez,A.J. and Tomari,Y. (2013) Poly(A)-specific ribonuclease mediates 3'-end trimming of argonaute2-cleaved precursor micromas. *Cell Rep.*, **5**, 715–726.
59. Katoh,T., Hojo,H. and Suzuki,T. (2015) Destabilization of microRNAs in human cells by 3′

deadenylation mediated by PARN and CUGBP1. *Nucleic Acids Res.*, **43**, 7521–7534.
60. Chatterjee,S., Grosshans,H. and Großhans,H. (2009) Active turnover modulates mature microRNA activity in Caenorhabditis elegans. *Nature*, **461**, 546–549.
61. Bossé,G.D., Rüegger,S., Ow,M.C., Vasquez-Rifo,A., Rondeau,E.L., Ambros,V.R. and Simard,M.J. (2013) The decapping scavenger enzyme DCS-1 controls microRNA levels in Caenorhabditis elegans. *Mol. Cell*, **50**, 281–287.
62. Haas,G., Cetin,S., Messmer,M., Chane-Woon-Ming,B., Terenzi,O., Chicher,J., Kuhn,L., Hammann,P. and Pfeffer,S. (2016) Identification of factors involved in target RNA-directed microRNA degradation. *Nucleic Acids Res.*, **44**, 2873–87.
63. Elbarbary,R.A., Miyoshi,K., Myers,J.R., Du,P., Ashton,J.M., Tian,B. and Maquat,L.E. (2017) Tudor-SN–mediated endonucleolytic decay of human cell microRNAs promotes G_1/S phase transition. *Science (80-.).*, **356**, 859–862.
64. Tang,W., Tu,S., Lee,H.C., Weng,Z. and Mello,C.C. (2016) The RNase PARN-1 Trims piRNA 3′ Ends to Promote Transcriptome Surveillance in C. elegans. *Cell*, **164**, 974–984.
65. Lehrbach,N.J., Castro,C., Murfitt,K.J., Abreu-Goodger,C., Griffin,J.L. and Miska,E.A. (2012) Post-developmental microRNA expression is required for normal physiology, and regulates aging in parallel to insulin/IGF-1 signaling in C. elegans. *RNA*, **18**, 2220–2235.
66. Dexheimer,P.J., Wang,J. and Cochella,L. (2020) Two MicroRNAs Are Sufficient for Embryonic Patterning in C. elegans. *Curr. Biol.*, **30**.
67. Gantier,M.P., McCoy,C.E., Rusinova,I., Saulep,D., Wang,D., Xu,D., Irving,A.T., Behlke,M.A., Hertzog,P.J., Mackay,F., *et al.* (2011) Analysis of microRNA turnover in mammalian cells following Dicer1 ablation. *Nucleic Acids Res.*, **39**, 5692–5703.
68. Alvarez-Saavedra,E. and Horvitz,H.R. (2010) Many families of C. elegans microRNAs are not essential for development or viability. *Curr. Biol.*, **20**, 367–373.
69. Ruby,J.G., Jan,C.H. and Bartel,D.P. (2007) Intronic microRNA precursors that bypass Drosha processing. *Nature*, **448**, 83–86.
70. Chung,W.-J., Agius,P., Westholm,J.O., Chen,M., Okamura,K., Robine,N., Leslie,C.S. and Lai,E.C. (2011) Computational and experimental identification of mirtrons in Drosophila melanogaster and Caenorhabditis elegans. *Genome Res.*, **21**, 286–300.
71. Westholm,J.O., Ladewig,E., Okamura,K., Nicolas,R. and Lai,E.C. (2012) Common and distinct patterns of terminal modifications to mirtrons and canonical microRNAs. *RNA*, **18**, 177–192.
72. Miki,T.S., Rüegger,S., Gaidatzis,D., Stadler,M.B. and Großhans,H. (2014) Engineering of a conditional allele reveals multiple roles of XRN2 in Caenorhabditis elegans development and substrate specificity in microRNA turnover. *Nucleic Acids Res.*, **42**, 4056–4067.
73. McJunkin,K. and Ambros,V. (2014) The embryonic mir-35 family of microRNAs promotes multiple aspects of fecundity in Caenorhabditis elegans. *G3 (Bethesda).*, **4**, 1747–1754.
74. Sherrard,R., Luehr,S., Holzkamp,H., McJunkin,K., Memar,N. and Conradt,B. (2017) Mirnas cooperate in apoptosis regulation during c. Elegans development. *Genes Dev.*, **31**, 209–222.
75. McJunkin,K. and Ambros,V. (2017) A microRNA family exerts maternal control on sex determination in C. elegans. *Genes Dev.*, **31**, 422–437.
76. Benner,L.K., Prothro,K.P. and McJunkin,K. (2019) The mir-35 family links maternal germline sex to embryonic viability in caenorhabditis elegans. *G3 Genes, Genomes, Genet.*, **9**, 901–909.
77. Yang,B. and McJunkin,K. (2020) CRISPR screening strategies for microRNA target identification. *FEBS J.*, **287**, 2914–2922.
78. Yang,B. and McJunkin,K. (2020) The mir-35-42 binding site in the nhl-2 3'UTR is dispensable for development and fecundity. *microPublication Biol.*

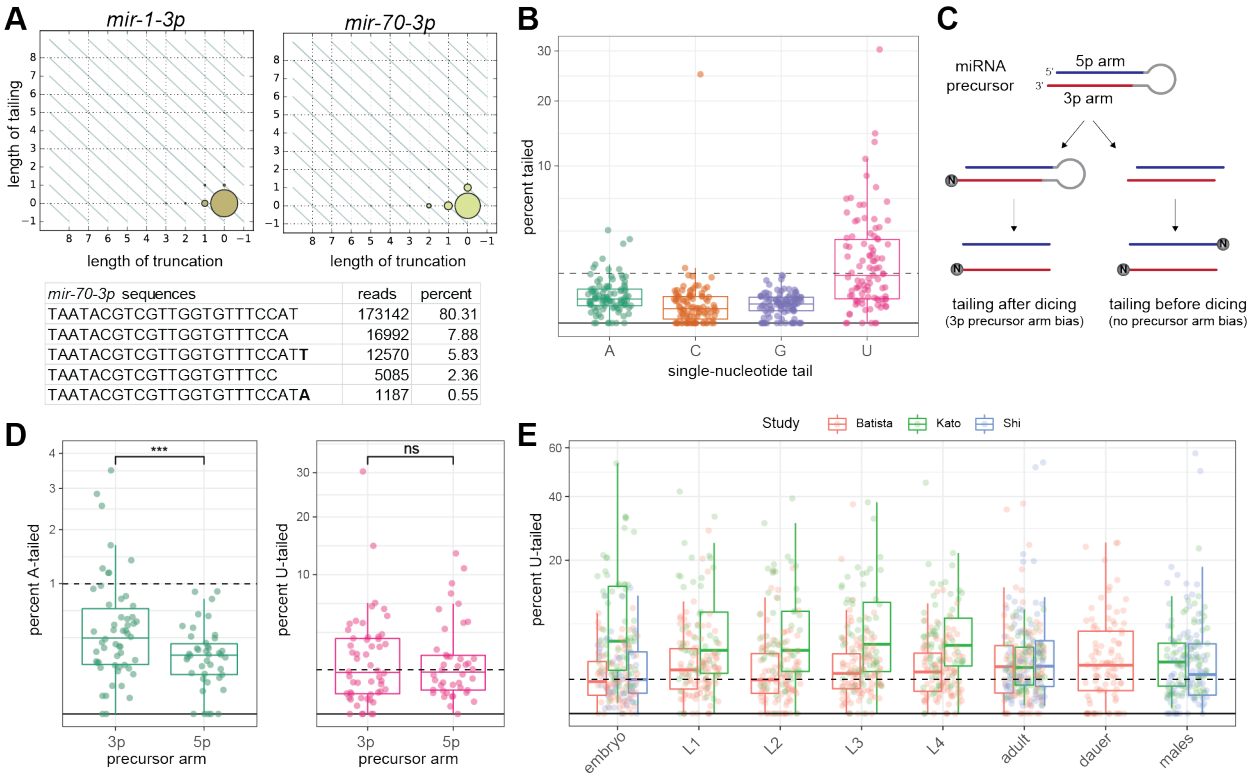

mir-70-3p sequences	reads	percent
TAATACGTCGTTGGTGTTTCCAT	173142	80.31
TAATACGTCGTTGGTGTTTCCA	16992	7.88
TAATACGTCGTTGGTGTTTCCAT**T**	12570	5.83
TAATACGTCGTTGGTGTTTCC	5085	2.36
TAATACGTCGTTGGTGTTTCCAT**A**	1187	0.55

Figure 1. Characterization of miRNA tailing in *C. elegans*. A) 2D matrix representing the truncation and tailing status of the indicated miRNAs. The sizes of the dots represent the proportion of reads, with the canonical sequence at zero on both axes, and increasingly trimmed or tailed species plotted to the left on the x-axis or upward on the y-axis, respectively. Bottom: Number of reads of most abundant *mir-70-3p* species in one wild type adult library, with the canonical sequence being the most abundant. B) Prevalence of single nucleotide 3' terminal additions of each indicated nucleotide in one biological replicate. C) Schematic of miRNA tailing preceding or following Dicer-mediated cleavage of the miRNA precursor. D) Comparison of prevalence of mono-adenylation and mono-uridylation on 3p- versus 5p-derived miRNAs. One biological replicate is shown. *p*-value from Fisher's exact test on three pooled biological replicates, ***<0.0001. E) Meta-analysis of three published datasets shows tailing across *C. elegans* developmental stages. Prevalence of mono-uridylation of miRNAs across development is shown. Only miRNAs with >50 RPM in the indicated library were analyzed. B, D) Only miRNAs with > 50RPM in all biological replicates were analyzed. B, D-E) Each dot represents an individual miRNA.

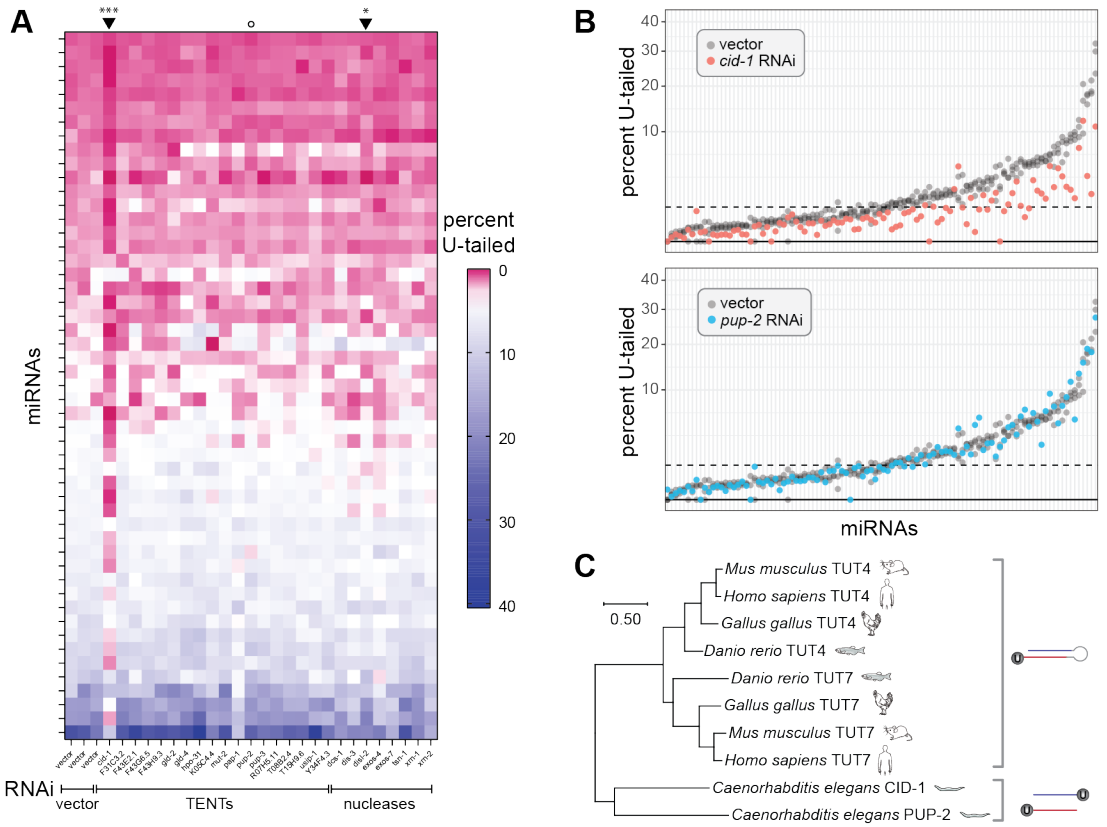

Figure 2. miRNA uridylation requires CID-1. A) Heatmap summarizing percent of mono-uridylation across each miRNA in each RNAi condition. All miRNAs with >50 RPM in all empty vector replicates and an average of >1% mono-uridylation across the three empty vector replicates are shown. Arrowhead above heatmap indicates column significantly different than vector (*cid-1* and *exos-4* RNAi). ***p-value = 0.0003, * p-value = 0.016. Open circle indicates *pup-2* RNAi, which does not have an effect. B) Percent mono-uridylation in vector or indicated RNAi. Each column is an individual miRNA. All miRNAs with >50 RPM in all empty vector replicates are shown. Three biological replicates of empty vector are shown in gray. C) Phylogenetic relationship of CID-1, PUP-2, TUT4, and TUT7. (Note the following alternative names for these genes CID-1/CDE-1/PUP-1, PUP-2, TUT4/TENT3A/ZCCHC11/PAPD3, and TUT7/TENT3B/ZCCHC6/PAPD6.)

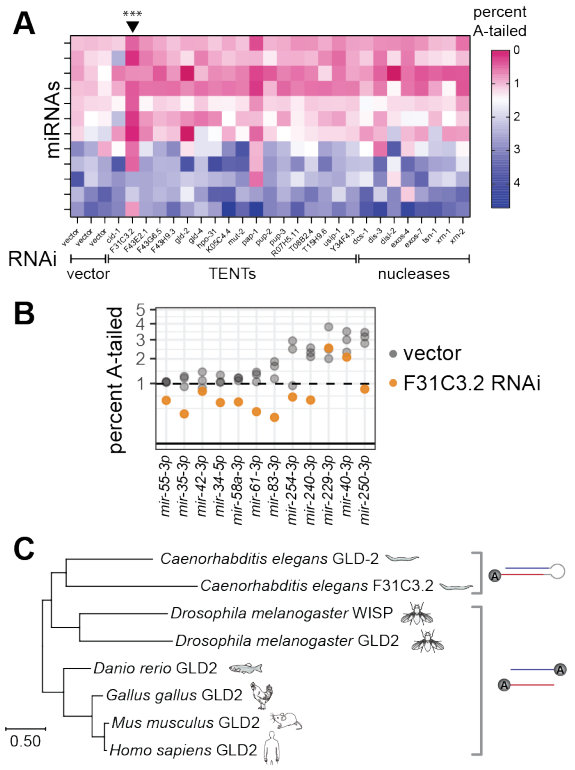

Figure 3. miRNA adenylation requires F31C3.2/GLDR-2. A) Heatmap summarizing percent of mono-adenylation across each miRNA in each RNAi condition. Arrowheads above heatmap indicate columns significantly different from vector, corresponding to F31C3.2 RNAi, which each reduces adenylation. ***p-value = 0.0003 B) Percent mono-adenylation in vector or F31C3.2/GLDR-2 RNAi. Three biological replicates of empty vector are shown in gray. A-B) All miRNAs with >50 RPM in all empty vector replicates and an average of >1% mono-adenylation across the three empty vector replicates are shown. C) Phylogenetic tree of F31C3.2/GLDR-2, GLD-2, and WISP. (Note that GLD2 in humans is also known as TENT2/TUT2/PAPD4/APD4.)

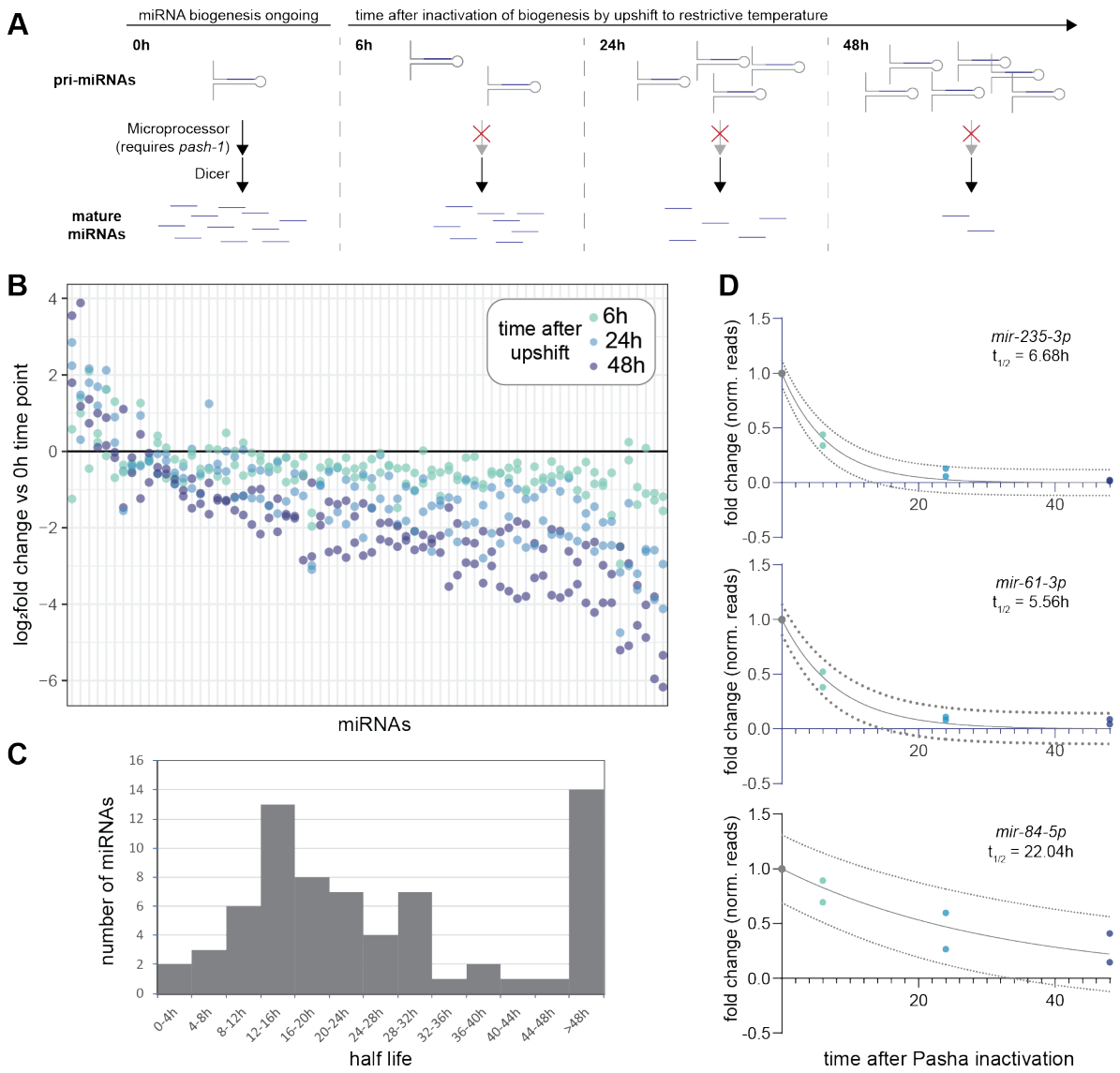

Figure 4. Characterization of miRNA half lives in *C. elegans*. A) Schematic of time courses after *pash-1* inactivation used for measuring miRNA decay. B) Log_2 fold change of miRNA reads compared to 0h after PASH-1 inactivation. Reads are normalized to spike-ins. C) Distribution of miRNA half-lives modeled from *pash-1(ts)* time course data. D) Representative time course data plotted as fold change, with exponential decay model and 95% prediction bands (dashed lines). (B-D) Only miRNAs with >50RPM in both replicates at the 0h timepoint were included in the analysis.

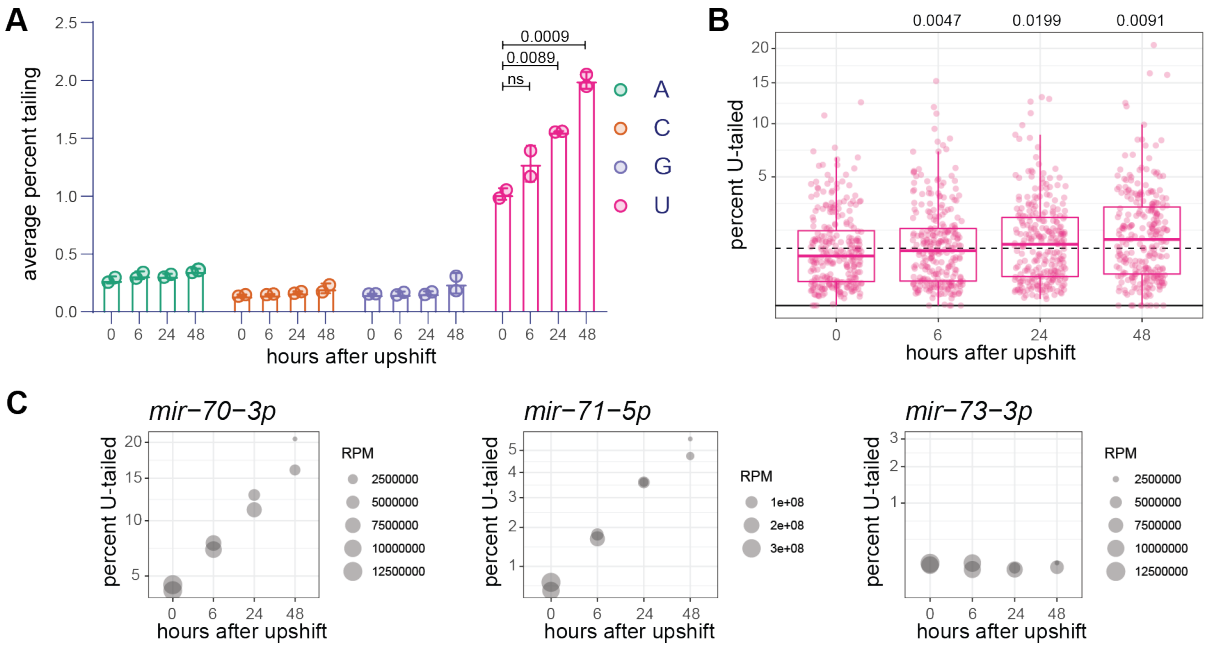

Figure 5. miRNA tailing correlates with miRNA age. A) Average percent of reads bearing each indicated single-nucleotide tail. B) Prevalence of mono-uridylation of miRNAs across time course after PASH-1 inactivation in one biological replicate. Each dot represents an individual miRNA. A-B) One-way ANOVA was used to compare all time points to 0h; when ANOVA was significant, Dunnett's multiple comparison test was performed, and *p*-values are shown above graph. C) Representative plots for indicated miRNAs, where y-axis indicates percent mono-uridylation, and size of dot represents read number. Note that reads here are reads per million spike-in reads, an arbitrary unit.

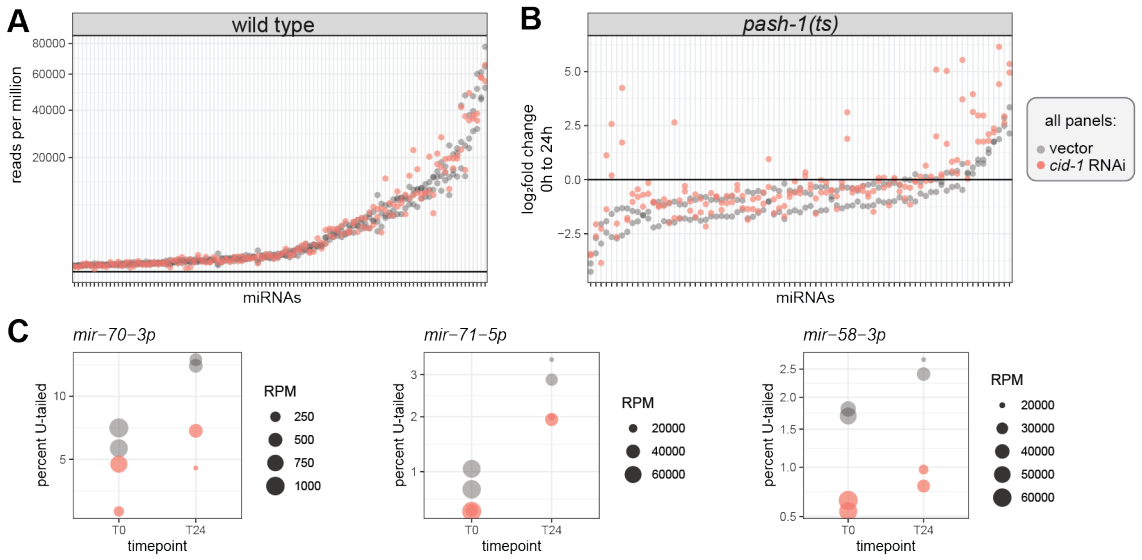

Figure 6. Uridylation does not globally regulate miRNA abundance or decay. (A-B) Each column is an individual miRNA. A) Abundance of miRNAs in empty vector or *cid-1* RNAi (pink). B) Log_2fold change from zero to 24h after PASH-1 inactivation. Each miRNA with >50 RPM at 0h in both empty vector replicates is shown. C) Plots showing percent mono-uridylation and miRNA abundance at zero and 24h after PASH-1 inactivation. Size of dot represents abundance, and y-axis is percent mono-uridylation. (A-C) Two independent biological replicates are shown.